Electronic supplementary information

New Journal of Chemistry

Electrochemical Sensor Based on Polyoxometalate Immobilized Using a Layer by Layer Assembly Process to Detect 2,4-Dinitrophenylhydrazine

Xiaoxia Yu, Jianye Pei, Lihua Bi*

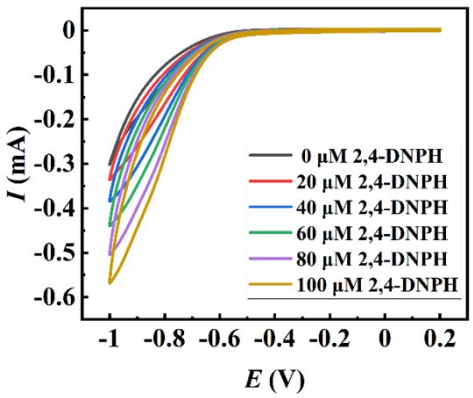

Fig. S1 CV curves of bare ITO in 0, 40, 60, 80, 100 μM 2,4-DNPH solution (pH 3.0) at scan rate of 50 $mV \cdot s^{-1}$.

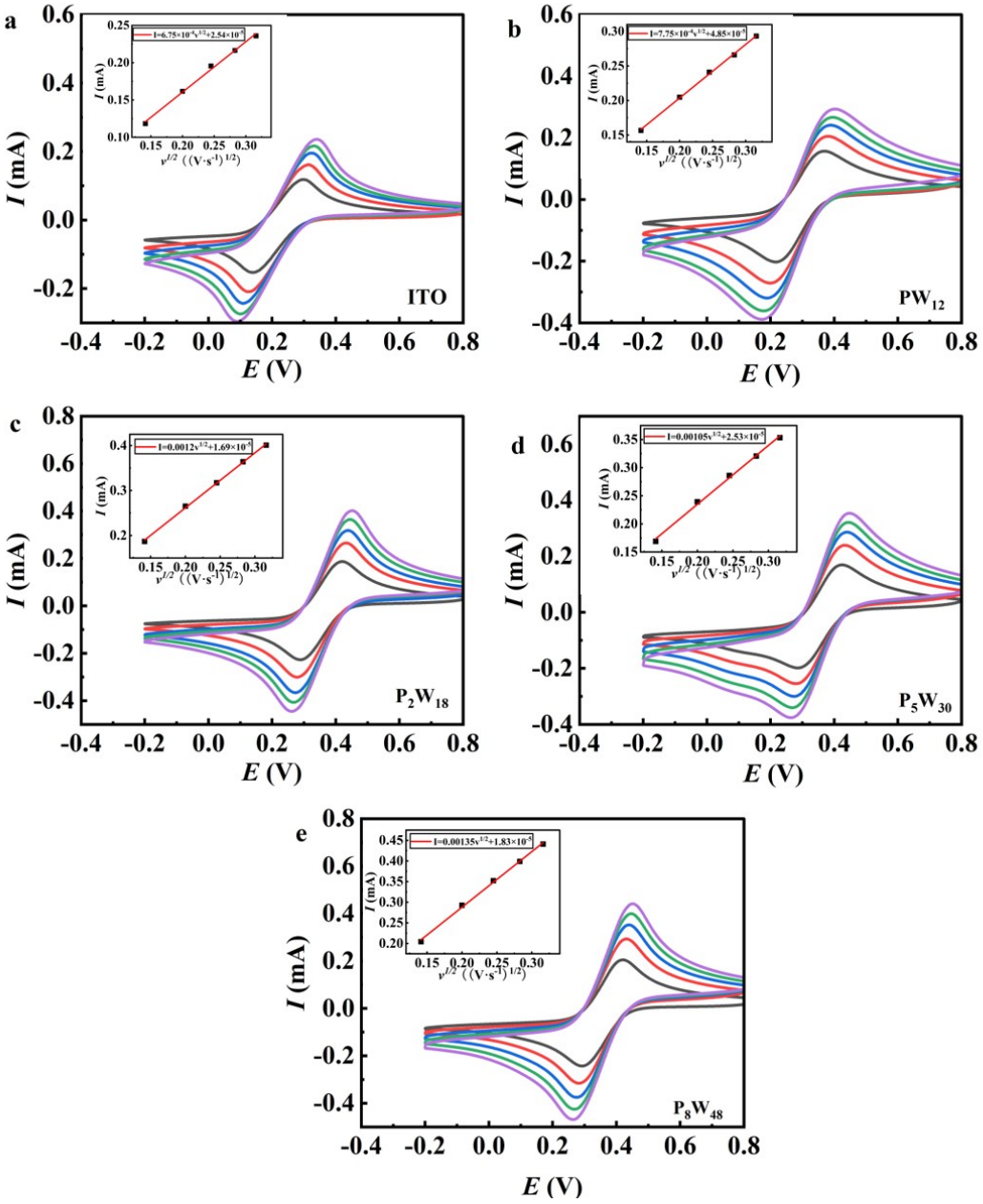

Fig. S2 CV curves of the bare ITO, $(PW_{12}/PDDA)_6$, $(P_2W_{18}/PDDA)_6$, $(P_5W_{30}/PDDA)_6$ and $(P_8W_{48}/PDDA)_6$ electrode in the mixture solution of 1.0 mM $[Fe(CN)_6]^{3-/4-}$ and 0.1 M KCl with different scan rates from 20 to 100 $mV \cdot s^{-1}$ and the linear relationship between the peak current and the square root of the scan rates at 0.4 V.

Fig. S3 CV curves of $(PW_{12}/PDDA)_6$(a), $(P_2W_{18}/PDDA)_6$(b), $(P_5W_{30}/PDDA)_6$(c), $(P_8W_{48}/PDDA)_6$(d) in 0.5 M sodium sulfate solution (pH 3.0) at scan rate of 50 $mV \cdot s^{-1}$.

Fig. S4 (a) CV curves of P_8W_{48} in solution (pH 7.0) at different scan rates from 10 to 100 $mV \cdot s^{-1}$ and (b) the linear relationship between the peak currents and the square roots of the scan rates; (c) CV curves of $(P_8W_{48}/PDDA)_7$ in solution (pH 7.0) with different scan rates from 10 to 100 $mV \cdot s^{-1}$ and (d) the linear relationship between the peak currents and the scan rates.

Fig. S5. (a**)** CV curves of $(P_8W_{48}/PDDA)_7$ modified electrode at the different concentrations of 2,4-DNPH (0, 20, 40, 60, 80, 100 μM) using the scan rate of 50 $mV \cdot s^{-1}$ and (b) its linear relationship between the reduction peak currents at -0.68 V and the concentrations of 2,4-DNPH.

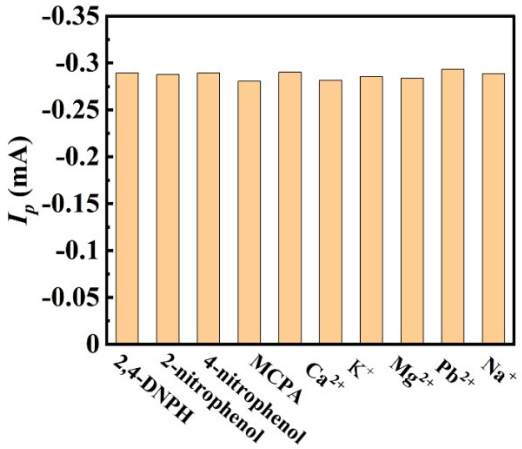

Fig. S6 Chart of $(P_8W_{48}/PDDA)_7$ modified electrode in 20 μM 2,4-DNPH solution with 40 μM 2-nitrophenol, 4-dinitrophenol, 4-chloro-2-methylphenol, Ca^{2+}, K^+, Mg^{2+}, Pb^{2+} or Na^+ at pH 7.0.

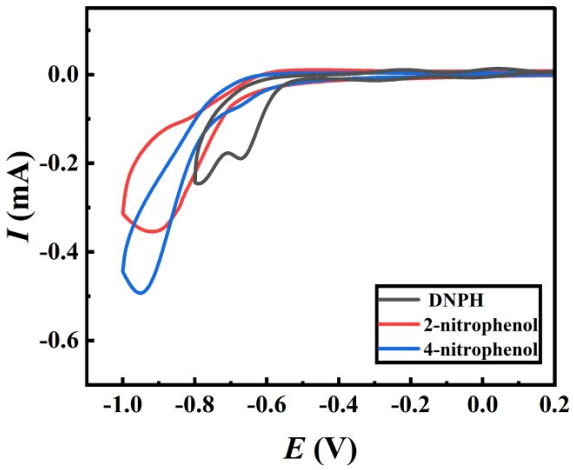

Fig. S7 CV curves of $(P_8W_{48}/PDDA)_6$ in 20 μM 2,4-DNPH, 40 μM 2-nitrophenol and 40 μM 4-dinitrophenol without(a) and with(b) , pH=7, 50mV/s.

Fig. S8 (a) Chart showing reduction peak current value recorded at -0.68 V in 20 μM 2, 4-DNPH for ten consecutive readings; (b) chart showing reduction peak current value recorded at -0.68 V in 20 μM 2, 4-DNPH using five different $(P_8W_{48}/PDDA)_7$ modified electrodes; (c) CV curves of $(P_8W_{48}/PDDA)_7$ modified electrode in blank buffer solution (pH 7.0) during 100 scanning cycles at scan rate of 50 $mV \cdot s^{-1}$.

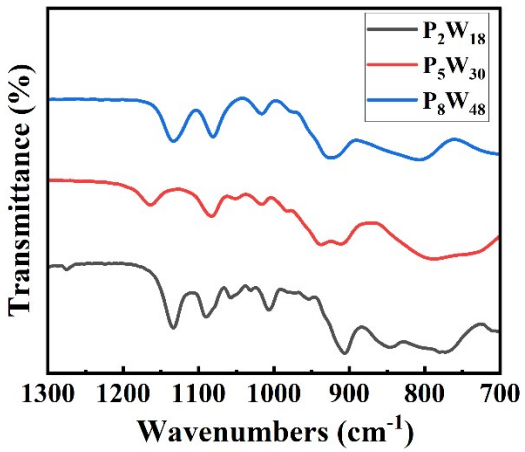

Fig. S9 IR spectra of P_2W_{18}, P_5W_{30} and P_8W_{48} in KBr pellets.

Table S1. Comparison of the electrocatalytic performance of four POMs in the solution for the reduction of 2,4-DNPH (100 μM) at scan rate of 50 $mV \cdot s^{-1}$.

No.	POM	Ep(V)	ΔI(mA)

a	PW_{12}	-0.6	0.326
b	P_2W_{18}	-0.48	0.216
c	P_5W_{30}	-0.57	0.388
d	P_8W_{48}	-0.50	0.399

Table S2. Comparison of the reduction potential (the potential value at which the catalytic current reaches the maximum value when the modified electrode catalyzes 2,4-DNPH) and CAT of four POMs modified electrode in pH 3.0 solution containing 0 to 100 μM of 2,4-DNPH at scan rate of 50 $mV \cdot s^{-1}$.

No.	Modified electrode	Reduction potential (V)	CAT(%)
a	$(PW_{12}/PDDA)_6$	-0.68	493.2
b	$(P_2W_{18}/PDDA)_6$	-0.66	635.1
c	$(P_5W_{30}/PDDA)_6$	-0.76	255.0
d	$(P_8W_{48}/PDDA)_6$	-0.61	1172.9